

Effect of SiO₂ Nanoparticles on Thermal Properties of Polyaniline/ Palmitic Acid Composite as an Energy Storage System

Shahmoradi, Ali Reza; Vakili, Mohammad Hassan⁺; Ghahremani, Parastoo*
Department of Chemical Engineering, Shahreza Branch, Islamic Azad University, Shahreza, I.R. IRAN

ABSTRACT: Phase Change Materials (PCMs) can be used as thermal energy storage systems in the form of latent heat. These materials are commonly enclosed in a suitable container, in order to prevent leakage of the molten PCM into the surrounding environment. In this study, palmitic acid and polyaniline were used as PCM and polymeric shell, respectively, to prepare a form stable composite. SiO₂ nanoparticle was added to the composite to improve thermal characteristics of the composite. The structure and morphology of the prepared form stable nanocomposite were investigated by Fourier Transform InfraRed (FT-IR) spectroscopy, Field Emission Scanning Electron Microscopy (FE-SEM), and X-Ray Diffractometer (XRD) tests. It was found that the synthesized nanocomposite was fabricated in the form of relatively smooth and compact spherical particles with a size of about 500 nm. Thermal properties of the prepared nanocomposite containing different concentrations of SiO₂ nanoparticles were determined using Differential Scanning Calorimetry (DSC) and Thermo Gravimetric Analysis (TGA) tests. It was found that the melting temperature and thermal conductivity of the polyaniline/palmitic acid composite increased by about 16% and 62%, respectively, when combined with 2 wt.% SiO₂ nanoparticles. The obtained results revealed that the polyaniline/palmitic acid/2 wt.% SiO₂ nanocomposite can be considered a suitable option for thermal energy storage applications.

KEYWORDS: Phase Change Material; Polyaniline; Form stable; Energy storage; Silica nanoparticle.

INTRODUCTION

In recent years, with regard to the increasing demands for energy storage systems due to the depletion of fossil resources, thermal energy storage systems have become a hot topic in related research. An effective way to store thermal energy is to use latent heat through Phase Change Materials (PCMs). These materials have relatively high latent heat of fusion and can absorb and store heat by melting and release the stored heat by freezing. Since

PCMs must be converted from solid to liquid during storage of thermal energy, they must be enclosed in a container to prevent leakage in the liquid state.

Nowadays, different investigations have been conducted in the field of preparation and application of a new system, called Form-Stable Phase Change Material (FS-PCM)[1–4]. These systems are a combination of PCM and a preservative-based substance such as an organic or

* To whom correspondence should be addressed.

+ E-mail: mhvakili@iaush.ac.ir

1021-9986/2022/10/3304-3313

10/\$/6.00

inorganic agent that can be used directly for a variety of applications without additional equipment. Due to the fact that the porosity of inorganic materials is usually high, PCMs are included in these pores to achieve stable systems. These products are commonly used for efficient storage of thermal energy in building materials. [5]. thus, various researches have been done in this field and different inorganic materials such as kaolin [6], diatomite [7–9], expanded perlite [10–13], and vermiculate [9,14], have been used as the preserving-based material in FS-PCMs. *Karaipekly & Sari*[15] prepared capric acid (CA)–meristic acid (MA) eutectic mixture/vermiculite (VMT) composite as a form-stable PCM. They reported that the eutectic mixture could enter the vermiculate pores up to 20 %wt., without any seepage during the melting process. The form-stable composite also showed good thermal and chemical stability. Sun et al. [7] prepared a composite of paraffin as the phase change material and calcined diatomite as the carrier materials. They found that the latent heat of the prepared composite was about 89.54 J/g under optimal conditions. Expanded perlite/octadecanol was another composite used by Peizhao et al. as FS-PCM [16]. Expanded graphite (EG) was used in the nanocomposite as a leakage reducing agent and the results showed that the latent heat capacity and phase change temperature of the nanocomposite containing 15% EG are 140.20 J/g and 59 °C, respectively.

Some polymers have been used as organic-based materials such as: methyl methacrylate methacrylic acid copolymer[17], polyvinyl chloride [17], epoxy resin [18], poly (styrene-methyl methacrylate) [19], acrylic polymers [20], polyethylene terephthalate[21,22], polyurethane [23] and polymethyl methacrylate[24,25], poly (melamine-formaldehyde)[26], poly (urea-formaldehyde) [27], and polyaniline [28–30].

Sari [31] studied an FS-PCM system consisting of paraffin as PCM and high-density polyethylene as supporting material. The study revealed that a form stable composite with a maximum of 77 wt. % of paraffin could be formed without any seepage in the melted state. A good dispersion of PCM in the polymer bulk was also observed in the results of this research.

A serious drawback of PCMs in practical applications is their low thermal conductivity, which can affect the amount of heat energy stored and released and reduce PCM performance. The use of nanomaterials in PCM

energy storage systems is an effective way to increase the thermal conductivity of these systems. Different types of nanoparticles, such as carbon nanotubes [32–34], TiO₂ nanoparticles[35,36], Ag nanoparticles [37], and CuO nanoparticles [38] have been investigated for this purpose. *Yi et al.* [39] used two-dimensional montmorillonite nanosheets as a ultrathin shell to encapsulate stearic acid latex particles. Their results showed that the latent heat storage capacity and thermal conductivity of the prepared PCM are 184.88 J/g and 159.46%, respectively.

In the present work, using emulsion polymerization method, a stable phase change material including palmitic acid as core and polyaniline as shell material was prepared and the effect of different concentrations of SiO₂ nanoparticles on the thermal properties of the produced nanocomposite was investigated.

EXPERIMENTAL SECTION

Materials

Aniline, sodium dodecyl sulfate, and ammonium persulfate were prepared from Merck Co. Palmitic acid was purchased from Panreac Química SLU, Spain. SiO₂ nanoparticle was purchased from Sigma Aldrich co.

Nanocomposite preparation

An emulsion polymerization method was conducted to prepare the form stable nanocomposite. For this purpose, 3 g of palmitic acid and 1-5 wt. % SiO₂ nanoparticles were added to 100 ml of water at 60 °C and stirred vigorously for 30 minutes to obtain a homogenous emulsion. Then 4 g of aniline was added to the mixture and stirred for another 30 minutes. After, 100 ml of aqueous solution of ammonium persulfate with a concentration of 100 g/lit as an oxidizing agent was added dropwise to the mixture for 30 min by syringe pump to complete the polymerization process. The mixture was then filtered and washed twice with ethanol to remove unreacted fatty acids. Finally, the obtained dark green powder was dried in an oven at 70 °C. Fig. 1 shows a schematic of the composite preparation process.

Characterization methods

Fourier transform infrared (FT-IR) spectrum of the synthesized nanocomposite was performed by a Perkin Elmer 1600 series Spectrophotometer, (MA, USA) in the wavelength range of 400 to 4000 cm⁻¹. X-ray diffraction (XRD)

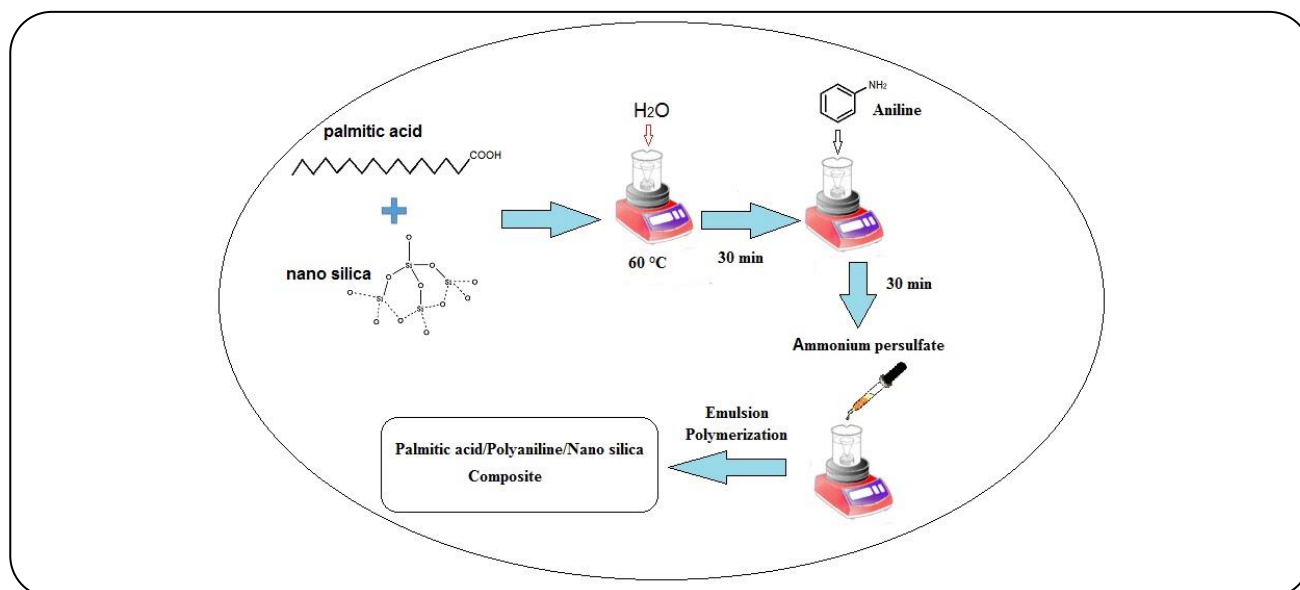


Fig. 1: schematic view of composite synthesized in the presence of silica nanoparticles.

patterns of the nanocomposites with different concentrations of SiO₂ nanoparticles were recorded using Philips X-ray spectrometer, PW 1800 type (Netherlands) with Cu K α radiation ($\lambda = 1.54060 \text{ \AA}$). Field Emission Scanning Electron Micrograph (FE-SEM) were taken with TESCAN MIRA3 instrument (Czech Republic) equipped with EDS spectrometer. ThermoGravimetric Analysis (TGA) was performed using SDTA 851e analyzer in the temperature range of 25 to 600 °C and heating rate of 5 °C/min under nitrogen atmosphere. Differential Scanning Calorimetry (DSC) analysis were performed using TA instrument from room temperature to 115 °C with a ramp of 10 °C/min under nitrogen atmosphere. To measure the thermal conductivity, the steady-state heat flow method was used at room temperature using DRX-II-RW Insulation Material thermal conductivity tester. For this purpose, the composite sample was milled and pressed under a pressure of 10 MPa to obtain a 20 mm tablet. Then one plate of tester was heated to 35 °C and the other plate was cooled to 15 °C with cold water. The tablet was then placed between two plates and its conductivity was measured.

RESULTS AND DISCUSSION

Structure and morphology characterization

The FT-IR spectrums of palmitic acid/polyaniline composite containing 2% wt. SiO₂ nanoparticle and without nanoparticles are shown in Fig. 2.

As shown in Fig. 2-a, for palmitic acid/polyaniline composite containing 2 wt. % of SiO₂ nanoparticle, the broad band that appears in the wave number range of 3000 to 3800 cm⁻¹ is related to the stretching vibration of O-H and N-H bonds in palmitic acid and polyaniline structures [40]. The peaks that centered at 2927 cm⁻¹ and 2860 cm⁻¹ are assigned to the asymmetric and symmetric stretching vibration of C-H bonds, respectively [41]. The sharp peak at 1733 cm⁻¹ is related to the stretching vibration of carboxylic groups (C=O) in palmitic acid [42]. The out of plane vibration of -NH bonds in the polyaniline structure can be observed at 1612 cm⁻¹ [43]. The peak that appears at 1452 cm⁻¹ is related to the deformation vibration of C-H bonds in the -CH₂ and -CH₃ groups [44]. The peaks of bending vibration of C-H bonds in the aliphatic structures and the stretching vibration of C-N bonds appeared at 1452 cm⁻¹ and 1201 cm⁻¹, respectively [45,46]. The appeared peaks at 1047 cm⁻¹ and 545 cm⁻¹ are attributed to the stretching and bending vibrations of O-Si-O bonds, respectively [47,48]. The appearance of these peaks confirms the presence of SiO₂ nanoparticles in the structure of the produced nanocomposite. It is seen from Fig. 2-b that the FTIR spectrum of palmitic acid /polyaniline composite without nanoparticle differ from that of the sample with nanoparticles in some peaks, specially in 1407 cm⁻¹ that is relating to O-Si-O bonds.

The surface morphology of pure polyaniline and palmitic acid/polyaniline composite containing 2 wt.% SiO₂ nanoparticle was evaluated by FE-SEM (Fig. 3).

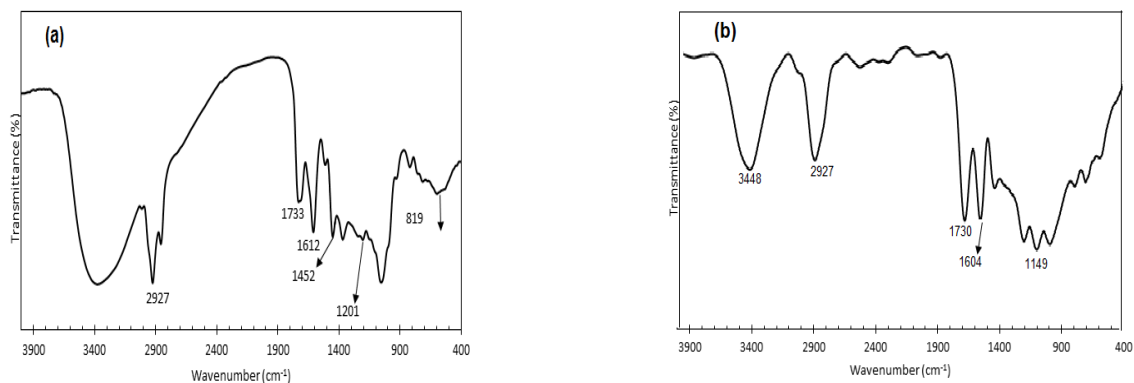


Fig. 2: FT-IR spectrum of (a) Palmitic acid/polyaniline composite containing 2% wt. SiO₂ nanoparticle (b) Palmitic acid/polyaniline composite without nanoparticle.

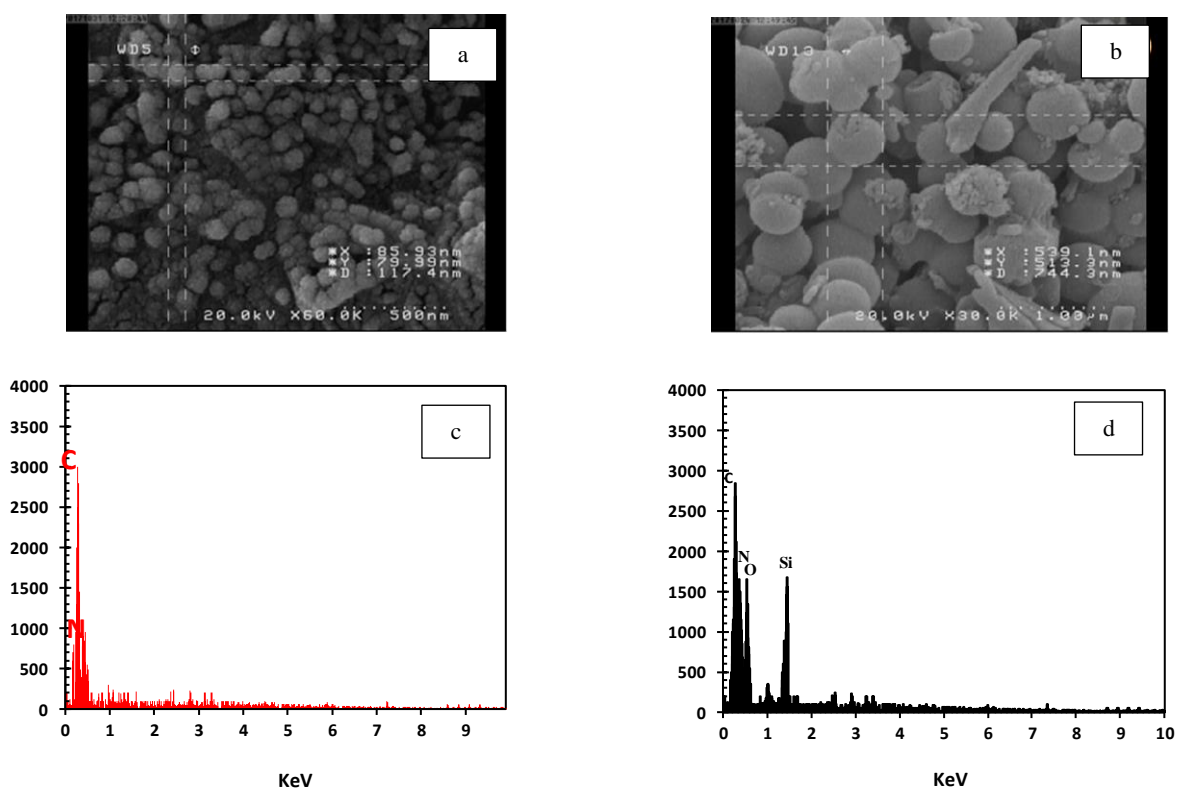


Fig. 3: FE-SEM and EDS results of (a, c) pure polyaniline and (b, d) palmitic acid/polyaniline composite containing 2% wt. SiO₂ nanoparticle

It can be seen from Fig. 3 (a) that the pure polyaniline sample has unspecified shape with a size of about 100 nm. While Fig. 3 (b) shows that the palmitic acid/polyaniline/SiO₂ nanocomposite is made in the form of sphere-like microcapsules with a diameter of about 500 nm. In addition, both samples are compact and have a relatively smooth

surface. EDS results revealed that only carbon and nitrogen were detected in the pure polyaniline sample. In contrast, the presence of carbon, nitrogen, oxygen, and silicon elements in the EDS results of the palmitic acid/polyaniline/SiO₂ sample, confirmed the presence of the silica nanoparticles in the produced nanocomposite.

In emulsion polymerization, first palmitic acid (dispersed phase) was distributed as fine particles in the solvent (continuous phase) and then aniline molecules surrounded the dispersed phase. Finally, polymerization was performed by adding a crosslinking agent. As a result, polyaniline and palmitic acid composites were synthesized as spherical particles. Fig. 4 shows the XRD patterns of palmitic acid (PA), polyaniline (PANI), palmitic acid/polyaniline composite (PA / PANI) and palmitic acid/polyaniline composite containing 2 wt. % SiO₂ nanoparticle.

In Fig. 4, The crystallographic peaks of palmitic acid correspond exactly to the peaks shown in other works [43,49]. The XRD pattern of polyaniline shows a wide peak typical for amorphous materials. It was also observed that the XRD PA / PANI pattern is very similar to the XRD pattern of palmitic acid with lower peak intensity. This may be due to the prevention of complete crystallization of palmitic acid by polyaniline molecules. This decrease in peak intensity is reported in another paper [43]. By adding SiO₂ nanoparticles to the palmitic acid / polyaniline composite, the intensity of XRD peaks of palmitic acid were reduced. Due to the low concentration of SiO₂ nanoparticles in the nanocomposite, the crystallographic peaks of nanosilica cannot be observed in the XRD pattern of the nanocomposite.

Thermal characterization

TGA/DTG diagrams of palmitic acid (PA), polyaniline (PANI), palmitic acid/polyaniline composite (PA/PANI) and palmitic acid/polyaniline composite containing 2 wt.% and 5 wt. % SiO₂ nanoparticle are shown in Fig. 5.

According to Fig. 5, polyaniline shows the highest thermal stability among the studied samples and its structure decomposes at about 393 °C, as previously reported by Zheng *et al.*[43]. The residual weight at 600 °C is about 62.3 wt. %.

The TGA curves also show that the structure of palmitic acid has the lowest thermal stability and its decomposition process begins at 260 °C. In polyaniline / palmitic acid composite, two stages of weight loss at 265 °C and 400 °C are observed, which are related to the decomposition of palmitic acid and polyaniline, respectively.

As shown in Fig. 5 (b), in samples containing 2% and 5% by weight of SiO₂ nanoparticles, the presence of

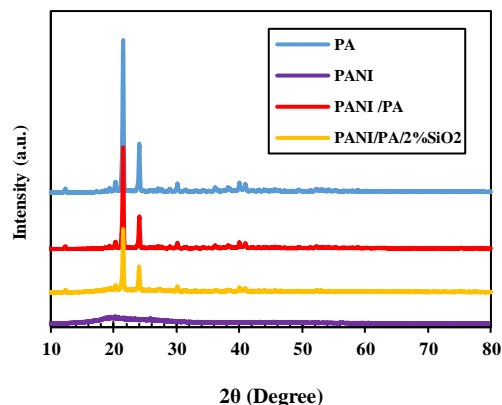


Fig. 4: XRD patterns of palmitic acid (PA), polyaniline (PANI), palmitic acid/polyaniline composite (PA/PANI), and palmitic acid/polyaniline composite containing 2% wt. SiO₂ nanoparticle.

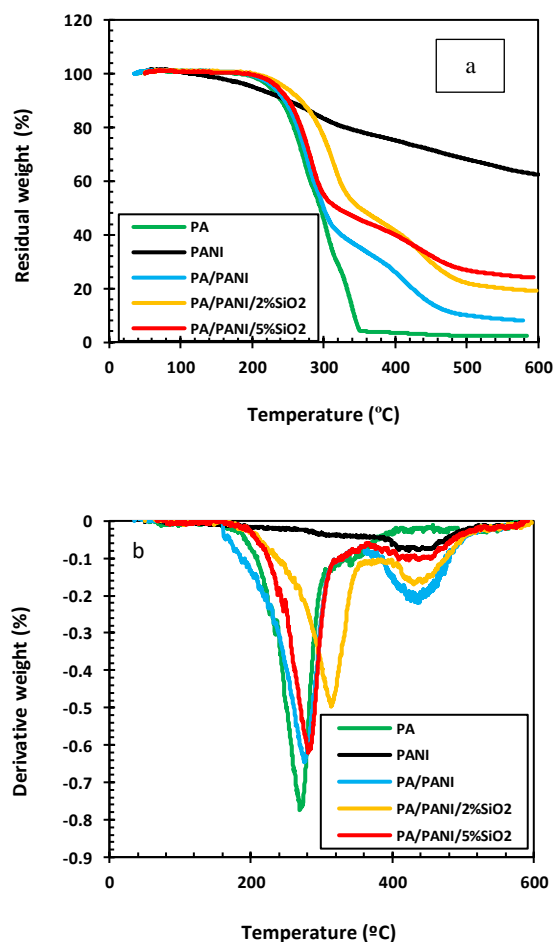
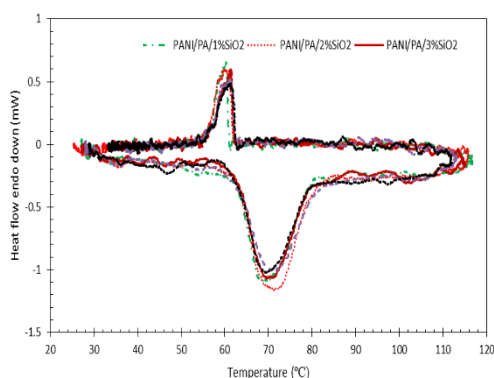


Fig. 5: (a) TGA and (b) DTG diagrams of palmitic acid (PA), polyaniline (PANI), palmitic acid/polyaniline composite (PA/PANI) and palmitic acid/polyaniline composite containing 2% wt. and 5% wt. SiO₂ nanoparticle

Table 1: Thermal properties of PANI/PA/SiO₂ nanocomposites containing different concentrations of the SiO₂ nanoparticles.

Compound	Melting Temperature (°C)	Latent Heat of Fusion (j/g)	Crystallization Temperature (°C)	Latent Heat of Crystallization (j/g)
PANI/PA/1% SiO ₂	68.86	70.75	60.30	15.08
PANI/PA/2% SiO ₂	71.93	75.38	59.69	17.46
PANI/PA/3% SiO ₂	70.25	74.46	59.26	14.91
PANI/PA/4% SiO ₂	71.01	61.42	61.26	15.23
PANI/PA/5% SiO ₂	69.8	73.15	61.34	14.82

**Fig. 6: DSC curves of the nanocomposites containing different concentrations of the SiO₂ nanoparticles.**

an endothermic peak in the range of 200-320 °C (the range of palmitic acid decomposition [49]), expresses the domination of palmitic acid in the nanocomposites, as also seen in the XRD results. The higher intensity of DTG peak in the nanocomposite containing 5 wt% of SiO₂, and also the maximum peak transfer to lower temperatures compared to the sample containing 2 wt% SiO₂, may be due to the higher thermal stability of palmitic acid/polyaniline/2% wt. SiO₂ nanocomposite. In other words, it can be concluded that SiO₂ nanoparticles agglomerate by increasing the concentration by more than 2% by weight, which leads to a decrease in the thermal stability of the nanocomposite. The next step in weight loss of samples containing nanoparticles, in the range of 350-500 °C, is attributed to the thermal decomposition of polyaniline chains [50].

DSC analysis was used to better investigate the effect of nanoparticle concentration on the thermal properties of nanocomposites. DSC curves of nanocomposites containing different concentrations of SiO₂ nanoparticles are presented in Fig 6 and the resulting parameters are reported in Table 1.

The melting point of palmitic acid is about 60 °C [51]. According to Table 1, the melting temperature of the prepared nanocomposites is at least about 16% higher than the pure palmitic acid. In addition, it can be observed that the highest melting temperature, as well as latent heat of fusion and crystallization, was obtained by incorporating 2% wt. of SiO₂ in the prepared nanocomposite. It may be due to the agglomeration of the nanoparticles in the more nanoparticle concentrations.

Thermal conductivity

Fig 7 shows the thermal conductivity of the used pure materials and the prepared nanocomposites. According to the results, the thermal conductivity of polyaniline/palmitic acid mixture is higher than pure palmitic acid and lower than pure polyaniline. In some other works, the same result was reported [43]. Addition of silica nanoparticles to the polyaniline / palmitic acid composite increased the thermal conductivity by about 62%, which is significant. Shen et al. Also added nanosilica to the polyvinyl acetate copolymer and found that SiO₂ nanoparticles could significantly increase the thermal conductivity of the nanocomposite [52]. In another research, Kochetov et al. used the SiO₂ nanoparticles to increase the thermal conductivity of an epoxy-based nanocomposite[53]. The thermal conductivity of silica is in the range of 0.7-1.7 W/m.K, which is at least twice as high as the thermal conductivity of palmitic acid / polyaniline composite. Therefore, an increase in the thermal conductivity of nanocomposites containing SiO₂ nanoparticles is expected.

In addition, Fig. 7 shows that increasing the nanosilica content from 2% to 5% did not have a significant effect on the thermal conductivity of the nanocomposite. It can be due to the agglomeration of nanoparticles in the nanocomposite containing more than 2% wt. SiO₂.

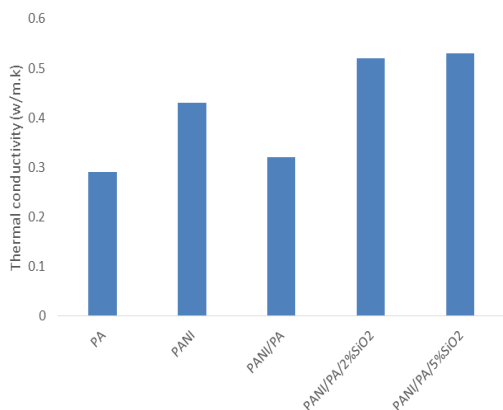


Fig. 7: Thermal conductivity of the used pure materials and the prepared nanocomposites.

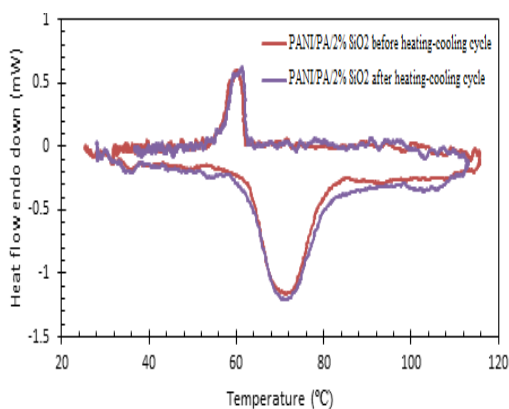


Fig. 8: Thermal stability of PANI/PA/2% SiO₂ nanocomposite.

Thermal and form stability

Thermal stability of the prepared nanocomposites was evaluated by 80 heating-cooling cycles of the nanocomposite containing 2 wt% SiO₂ nanoparticles. In Figure 8, the DSC curves of this nanocomposite are compared before and after the heating and cooling cycles. No significant difference was observed between the two samples, indicating the relative thermal stability of this composite.

In order to determine the form stability of the produced nanocomposites, PANI/PA/2% SiO₂ nanocomposite was weighed before and after exposure to a high temperature (75 °C) for 24 h. The weight loss was less than 1%, which indicate that the prepared nanocomposite was form stable.

CONCLUSIONS

In the present study, a form stable polyaniline/palmitic acid/SiO₂ nanocomposite was prepared and characterized

by morphological tests and thermal analysis. The fabricated nanocomposites were achieved in the form of spherical particles with a relatively smooth surface and size of about 500 nm. Different contents of SiO₂ nanoparticles were used to prepare composite. It was found that the melting temperature of the form stable nanocomposite is at least about 16% higher than pure palmitic acid. The highest melting temperature was observed in the nanocomposite containing 2 wt% of SiO₂ nanoparticles. In addition, it was found that the prepared form stable composite has good thermal stability and can be used in thermal energy storage systems in the range of melting point.

Received : Jul. 26, 2021 ; Accepted : Nov. 29, 2021

REFERENCES

- [1] Chen C., Liu W., Wang Z., Peng K., Pan W., Xie Q., **Novel form Stable Phase Change Materials Based on the Composites of Polyethylene Glycol/Polymeric Solid-Solid Phase Change Material**, *Solar Energy Materials and Solar Cells.*, **134**: 80–88 (2015).
- [2] Wen R., Zhang X., Huang Z., Fang M., Liu Y., Wu X., Min X., Gao W., Huang S., **Preparation and Thermal Properties of Fatty Acid/Diatomite Form-Stable Composite Phase Change Material for Thermal Energy Storage**, *Solar Energy Materials and Solar Cells.* **178**: 273–279 (2018).
- [3] Zeng J.-L., Chen Y.-H., Shu L., Yu L.-P., Zhu L., Song L.-B., Gao Z., Sun L.-X., **Preparation and Thermal Properties of Exfoliated Graphite/Erythritol/Mannitol Eutectic Composite as Form-Stable Phase Change Material for Thermal Energy Storage**, *Solar Energy Materials and Solar Cells.*, **178**: 84–90 (2018).
- [4] Sheng N., Nomura T., Zhu C., Habazaki H., Akiyama T., **Cotton-Derived Carbon Sponge as Support for Form-Stabilized Composite Phase Change Materials with Enhanced Thermal Conductivity**, *Solar Energy Materials and Solar Cells.*, **192**: 8–15 (2019).
- [5] Soares N., Costa J.J., Gaspar A.R., Santos P., **Review of Passive PCM latent Heat Thermal Energy Storage Systems Towards Buildings' Energy Efficiency**, *Energy and Buildings.*, **59**: 82–103 (2013).

- [6] Ali Memon S., Yiu Lo T., Shi X., Barbhuiya S., Cui H., Preparation, Characterization and Thermal Properties of Lauryl Alcohol/Kaolin as Novel Form-Stable Composite Phase Change Material for Thermal Energy Storage in Buildings, *Applied Thermal Engineering*, **59**: 336–347 (2013).
- [7] Sun Z., Zhang Y., Zheng S., Park Y., Frost R.L., Preparation and Thermal Energy Storage Properties of Paraffin/Calcined Diatomite Composites as Form-Stable Phase Change Materials, *Thermochimica Acta*, **558**: 16–21 (2013).
- [8] Karaman S., Karaipekli A., Sari A., Biçer A., Polyethylene glycol (PEG)/Diatomite Composite as a Novel Form-Stable Phase Change Material for Thermal Energy Storage, *Solar Energy Materials and Solar Cells*, **95**: 1647–1653 (2011)
- [9] Sari A., Biçer A., Thermal Energy Storage Properties and Thermal Reliability of Some Fatty Acid Esters/Building Material Composites as Novel Form-Stable PCMs, *Solar Energy Materials and Solar Cells*, **101**: 114–122 (2012).
- [10] Sari A., Karaipekli A., Preparation, Thermal Properties and Thermal Reliability of Capric Acid/Expanded Perlite Composite for Thermal Energy Storage, *Materials Chemistry and Physics*, **109**: 459–464 (2008).
- [11] Sari A., Karaipekli A., Alkan C., Preparation, Characterization and Thermal Properties of Lauric Acid/Expanded Perlite as Novel Form-Stable Composite Phase Change Material, *Chemical Engineering Journal*, **155**: 899–904 (2009).
- [12] Karaipekli A., Sari A., Capric–Myristic Acid/Expanded Perlite Composite as Form-Stable Phase Change Material for Latent Heat Thermal Energy Storage, *Renewable Energy*, **33**: 2599–2605 (2008).
- [13] Karaipekli A., Sari A., Preparation, Thermal Properties and Thermal Reliability of Eutectic Mixtures of Fatty Acids/Expanded Vermiculite as Novel Form-Stable Composites for Energy Storage, *Journal of Industrial and Engineering Chemistry*, **16**: 767–773 (2010).
- [14] Jeong S.-G., Jeon J., Cha J., Kim J., Kim S., Preparation and Evaluation of Thermal Enhanced Silica Fume by Incorporating Organic PCM, for Application to Concrete, *Energy and Buildings*, **62**: 190–195 (2013).
- [15] Karaipekli A., Sari A., Capric–Myristic Acid/Vermiculite Composite as Form-Stable Phase Change Material for Thermal Energy Storage, *Solar Energy*, **83**: 323–332 (2009).
- [16] Lv P., Ding M., Liu C., Rao Z., Experimental Investigation on Thermal Properties and Thermal Performance Enhancement of Octadecanol/Expanded Perlite Form Stable Phase Change Materials for Efficient Thermal Energy Storage, *Renewable Energy*, **131**: 911–922 (2019).
- [17] Sari A., Alkan C., Kolemen U., Uzun O., Eudragit S (Methyl Methacrylate Methacrylic Acid Copolymer)/Fatty Acid Blends as Form-Stable Phase Change Material for Latent Heat Thermal Energy Storage, *Journal of Applied Polymer Science*, **101**: 1402–1406 (2006).
- [18] Fang Y., Kang H., Wang W., Liu H., Gao X., Study on Polyethylene Glycol/Epoxy Resin Composite as a Form-Stable Phase Change Material, *Energy Conversion and Management*, **51**: 2757–2761 (2010).
- [19] Mohammadi Khoshraj B., Seyyed Najafi F., Mohammadi Khoshraj J., Ranjbar H., Microencapsulation of Butyl Palmitate in Polystyrene-Co-Methyl Methacrylate Shell for Thermal Energy Storage Application, *Iranian Journal of Chemistry and Chemical Engineering (IJCCCE)*, **37(3)**: 187-194 (2018).
- [20] Alkan C., Sari A., Uzun O., Poly(ethylene glycol)/Acrylic Polymer Blends for Latent Heat Thermal Energy Storage, *AIChE Journal*, **52**: 3310–3314 (2006).
- [21] Chen C., Wang L., Huang Y., Morphology and Thermal Properties of Electrospun Fatty Acids/Polyethylene Terephthalate Composite Fibers as Novel Form-Stable Phase Change Materials, *Solar Energy Materials and Solar Cells*, **92**: 1382–1387 (2008).
- [22] Chen C., Wang L., Huang Y., A Novel Shape-Stabilized PCM: Electrospun Ultrafine Fibers Based on Lauric Acid/Polyethylene Terephthalate Composite, *Materials Letters*, **62**: 3515–3517 (2008).
- [23] Sari A., Bicer A., Alkan C., Özcan A.N., Thermal Energy Storage Characteristics of Myristic Acid-Palmitic Eutectic Mixtures Encapsulated in PMMA shell, *Solar Energy Materials and Solar Cells*, **193**: 1–6 (2019).

- [24] Chananipoor A., Azizi Z., Raei B., Tahmasebi N., Synthesis and Optimization of GO/PMMA/n-Octadecane Phase Change Nanocapsules Using Response Surface Methodology, *Iranian Journal of Chemistry and Chemical Engineering (IJCCE)*, **40(2)**: 383-394 (2021)
- [25] Wang X., Li C., Zhao T., Fabrication and Characterization of Poly(Melamine-Formaldehyde)/Silicon Carbide Hybrid Microencapsulated Phase Change Materials with Enhanced Thermal Conductivity and Light-Heat Performance, *Solar Energy Materials and Solar Cells*, **183**: 82–91 (2018).
- [26] Vakili M.H., Jahanfar M., Microencapsulation of Butyl Stearate as Phase Change Material by Melamine Formaldehyde Shell for Thermal Energy Storage, *Journal of Chemical and Petroleum Engineering*, **51(2)**: 147-154 (2017).
- [27] Zhang K., Zhou Q., Ye H.-M., Optimizing the Preparation of Semi-Crystalline Paraffin/Poly(Urea-Formaldehyde) Microcapsules for Thermal Energy Storage, *Applied Sciences*, **9**: 599 (2019)
- [28] Yu C., Youn J.R., Song Y.S., Encapsulated Phase Change Material Embedded by Graphene Powders for Smart and Flexible Thermal Response, *Fibers and Polymers*, **20**: 545–554 (2019).
- [29] Fan S., Gao H., Xu Q., He H., Lu L., Shen J., et al., “Nanoencapsulation of n-Octadecane Phase Change Material with Polyaniline Shell for Thermal Energy Storage”, *Proceedings of the 3rd International Conference on Advances in Energy and Environmental Science*, Atlantis Press, Paris, France, (2015)
- [30] Zeng J.-L., Sun S.-L., Zhou L., Chen Y.-H., Shu L., Yu L.-P., et al., Preparation, Morphology and Thermal Properties of Microencapsulated Palmitic Acid Phase Change Material with Polyaniline Shells, *Journal of Thermal Analysis and Calorimetry*, **129**: 1583–1592 (2017).
- [31] Sari A., Form-Stable Paraffin/High Density Polyethylene Composites as Solid–Liquid Phase Change Material for Thermal Energy Storage: Preparation and Thermal Properties, *Energy Conversion and Management*, **45**: 2033–2042 (2004).
- [32] Karaipekli A., Biçer A., Sarı A., Tyagi V.V., Thermal Characteristics of Expanded Perlite/Paraffin Composite Phase Change Material with Enhanced Thermal Conductivity Using Carbon Nanotubes, *Energy Conversion and Management*, **134**: 373–381 (2017).
- [33] Kholmanov I., Kim J., Ou E., Ruoff R.S., Shi L., Continuous Carbon Nanotube–Ultrathin Graphite Hybrid Foams for Increased Thermal Conductivity and Suppressed Subcooling in Composite Phase Change Materials, *ACS Nano*, **9**: 11699–11707 (2015).
- [34] Tao Y.B., Lin C.H., He Y.L., Preparation and Thermal Properties Characterization of Carbonate Salt/Carbon Nanomaterial Composite Phase Change Material, *Energy Conversion and Management*, **97**: 103–110 (2015).
- [35] Masoumi H., Haghghi Khoshkhoo R., Mirfendereski S.M., Modification of Physical and Thermal Characteristics of Stearic Acid as a Phase Change Materials Using TiO₂-Nanoparticles, *Thermochimica Acta*, **675**: 9–17 (2019).
- [36] Motahar S., Alemrajabi A.A., Khodabandeh R., Experimental Study on Solidification Process of a Phase Change Material Containing TiO₂ Nanoparticles for Thermal Energy Storage, *Energy Conversion and Management*, **138**: 162–170 (2017).
- [37] Qian T., Li J., Min X., Guan W., Deng Y., Ning L., Enhanced Thermal Conductivity of PEG/Diatomite Shape-Stabilized Phase Change Materials with Ag Nanoparticles for Thermal Energy Storage, *Journal of Materials Chemistry A*, **3**: 8526–8536 (2015).
- [38] Ezhumalai D.S., Sriharan G., Harikrishnan S., Improved Thermal Energy Storage Behavior of CuO / Palmitic acid Composite as Phase Change Material, *Materials Today: Proceedings*, **5**: 14618–14627 (2018).
- [39] Yi H., Zhan W., Zhao Y., Qu S., Wang W., Chen P., et al., A Novel Core-Shell Structural Montmorillonite Nanosheets/Stearic Acid Composite PCM for Great Promotion of Thermal Energy Storage Properties, *Solar Energy Materials and Solar Cells*, **192**: 57–64 (2019).
- [40] Javidparvar A.A., Naderi R., Ramezanzadeh B., Bahlakeh G., Graphene Oxide as a pH-Sensitive Carrier for Targeted Delivery of Eco-Friendly Corrosion Inhibitors in Chloride Solution: Experimental and Theoretical Investigations, *Journal of Industrial and Engineering Chemistry*, **72**: 196–213 (2019).
- [41] Javidparvar A.A., Ramezanzade B., Ghasemi E., The “Effect of Oleic Acid/Silane Treatments of Fe₃O₄ Nanoparticles on the Mechanical Properties of an Epoxy Coating”, *The 6th International Color & Coating Congress, Institute for Color Science and Technology*, Tehran, (2015)

- [42] Javidparvar A.A., Naderi R., Ramezanzadeh B., Bahlakeh G., Graphene Oxide as a pH-Sensitive Carrier for Targeted Delivery of Eco-Friendly Corrosion Inhibitors in Chloride Solution: Experimental and Theoretical Investigations, *Journal of Industrial and Engineering Chemistry*, **72**: 176-213 (2019).
- [43] Zeng J.L., Zheng S.H., Yu S.B., Zhu F.R., Gan J., Zhu L., et al., Preparation and Thermal Properties of Palmitic Acid/Polyaniline/Exfoliated Graphite Nanoplatelets Form-Stable Phase Change Materials, *Applied Energy*, **115**: 603–609 (2014).
- [44] Shahmoradi A.R., Talebibahmanbigloo N., Javidparvar A.A., Bahlakeh G., Ramezanzadeh B., Studying the Adsorption/Inhibition Impact of the Cellulose and Lignin Compounds Extracted from Agricultural Waste on the Mild Steel Corrosion in HCl Solution, *Journal of Molecular Liquids*, **304**: 1-13 (2020).
- [45] Javidparvar A.A., Naderi R., Ramezanzadeh B., Designing a Potent Anti-Corrosion System Based on Graphene Oxide Nanosheets Non-Covalently Modified with Cerium/Benzimidazole For Selective Delivery of Corrosion Inhibitors on Steel in NaCl Media, *Journal of Molecular Liquids*, **284**: 415–430 (2019).
- [46] Javidparvar A.A., Ramezanzadeh B., Ghasemi E., Effect of Various Spinel Ferrite Nanopigments Modified by Amino Propyl Trimethoxy Silane on the Corrosion Inhibition Properties of the Epoxy Nanocomposites, *Corrosion*, **72(6)**: 761-774 (2016).
- [47] Javidparvar A.A., Ramezanzadeh B., Ghasemi E., Effects of Surface Morphology and Treatment of Iron Oxide Nanoparticles on the Mechanical Properties of an Epoxy Coating, *Progress in Organic Coatings*, **90**: 10-20 (2016).
- [48] Javidparvar A.A., Ramezanzadeh B., Ghasemi E., The Effect of Surface Morphology and Treatment of Fe₃O₄ Nanoparticles on the Corrosion Resistance of Epoxy Coating, *Journal of the Taiwan Institute of Chemical Engineers*, **61**: 356-366 (2016).
- [49] Mehrali M., Latibari S.T., Mehrali M., Indra Mahlia T.M., Cornelis Metselaar H.S., Preparation and Properties of Highly Conductive Palmitic Acid/Graphene Oxide Composites as Thermal Energy Storage Materials, *Energy*, **58**: 628–634 (2013).
- [50] Zong X., Cai Y., Sun G., Zhao Y., Huang F., Song L., Hu Y., Fong H., Wei Q., Fabrication and Characterization of Electrospun SiO₂ Nanofibers Absorbed with Fatty Acid Eutectics for Thermal Energy Storage/Retrieval, *Solar Energy Materials and Solar Cells*, **132**: 183–190 (2015)
- [51] Zeng J.L., Cao Z., Yang D.W., Xu F., Sun L.X., Zhang L., Zhang X.F., Phase Diagram of Palmitic Acid-Tetradecanol Mixtures Obtained by DSC Experiments, *Journal of Thermal Analysis and Calorimetry*, **95**: 501–505, (2009).
- [52] Shen M., Cui Y., He J., Zhang Y., Thermal Conductivity Model of Filled Polymer Composites, *International Journal of Minerals, Metallurgy, and Materials*, **18**: 623–631 (2011).
- [53] Kochetov R., Andritsch T., Lafont U., Morshuis P.H.F., Smit J.J., “Thermal Conductivity of Nano-Filled Epoxy Systems”, *Annual Report - Conference on Electrical Insulation and Dielectric Phenomena, CEIDP*, 658–661, (2009).